Endoscopic Tissue Characterization by Frequency-domain Fluorescence Lifetime Imaging (FD-FLIM)

J. MIZERET, G. WAGNIÈRES, T. STEPINAC, H. VAN DEN BERGH

Institute of Environmental Engineering, Swiss Federal Institute of Technology, Lausanne, Switzerland

Correspondence to J. Mizeret, Institute of Environmental Engineering, Swiss Federal Institute of Technology, CH-1015 Lausanne, Switzerland

Abstract. Tissue characterization by endoscopic fluorescence imaging of endogenous or exogenous fluorochromes is a promising method for early cancer detection. However, the steady-state fluorescence contrast between healthy tissue and lesions such as early-stage carcinomas is generally poor. The authors propose to improve this contrast by using the additional information contained in the fluorescence lifetime (FLT). The FLT of several fluorochromes is sensitive to their physico-chemical environment.

The FLT can be measured by frequency-domain methods. The excitation light from a continuous wave (CW) laser is modulated in amplitude at radio-frequencies by an electro-optic modulator, and delivered to the tissue via an optical fibre. The endoscopic site is imaged by an endoscope on to an optical device. The gain of the fluorescence image detector is also modulated at the same frequency for homodyning. The tissue fluorescence image is recorded at several phases between the excitation and the detection modulations during an acquisition cycle. With these images, an image processor calculates the apparent FLT for each pixel and constructs a lifetime image of the endoscopic site. This process is performed at quasi-video frequencies.

The influence of various physical parameters (modulation frequency, number of images by cycle, shot noise, tissue optical properties etc.) has been investigated by analytical analysis, simulation methods and experimentation.

Preliminary results obtained on human tissues are also presented to illustrate the potentiality of the method.

INTRODUCTION

Cancer continues to be a major health problem worldwide. In Western countries, one in three people will eventually develop cancer; one in five will die of the disease. As most of the advanced cancers are difficult to treat effectively, it is important to detect them at an early stage. Many invasive cancers are preceded by pre-malignant lesions such as dysplasia or early-stage tumours like carcinoma in situ. Unfortunately, most of these early-stage lesions are difficult to detect using standard techniques.

Moreover, many tumours originate in tissues lining the surface of hollow organs. Improvements in medical endoscopes allow investigation of most of these organs like the oesophagus, the upper aero-digestive tract, the tracheo-bronchial tree, the bladder, the colon and the female reproductive organs. Therefore, investigating these tissues by a sensitive method like fluorescence endoscopy is of particular interest.

Endoscopic tissue characterization has different applications such as localization of a suspected tumour, precise demarcation of the spreading of a tumour (1), control after therapy etc.

The principle of tissue characterization by fluorescence is to detect an optical contrast between the diseased tissue and the healthy surrounding area (2). Such a contrast in the fluorescence signal can be due to an alteration of the native fluorescence of tissues (endogenous fluorescence) (3, 4). Tissues are made

up of proteins, nucleic acids, lipids and water, and contain fluorescing and non-fluorescing chromophores. Many tissues are known to fluoresce in the ultra-violet and visible part of the spectrum. This fluorescence is notably due to natural fluorophores such as flavins, tryptophan, tyrosine, NADH, collagen, porphyrins, elastin and phenylalanine.

This optical contrast can also be enhanced by the application of an exogenous fluoro-chrome that localizes somewhat selectively in the diseased tissue (exogenous fluorescence) (5). These fluorochromes are usually photo-sensitizers used for photodynamic therapy (mTHPC, HPD, BPD etc.) but can also be applied for the purpose of photodetection only (5-ALA-induced PPIX, fluorescein, indocyanin green, monoclonal antibody-fluorochrome conjugates etc.).

Up to now, most of the studies in this field were based on steady-state fluorescence, and the contrast between normal and diseased tissue was based on the fluorescence intensity (5–10). This contrast can result from: a different concentration of natural or exogenous fluorochromes in the tissue; a change in the architecture of the tissues that alters the propagation of light (eg thickening of the epithelium); or a change in the physico-chemical environment of the fluorochrome that results in a different fluorescence quantum yield or in a shift of the emission and/or excitation wavelengths. For example, flavins and NADH are known to exhibit spectral changes when transforming from the oxidized to the reduced state.

These intensity-based methods are known to have several drawbacks. The difference of tissue optical properties at excitation and emission wavelengths requires complicated methods using two excitation and/or emission wavelengths for correction (11, 12). Another drawback is the small intensity contrast, which is difficult to extract from the noise inherent in the weak fluorescence signal. Moreover, these techniques are very sensitive to differences in the excitation light intensity due to the non-homogeneity of the illumination and to the complex geometry of the organs investigated.

Another approach is to measure the fluorescence lifetime (FLT) contrast of the tissue investigated. Typical FLTs of biological molecules range from tens of picoseconds (ps) to tens of nanoseconds (ns). Fluorescence decay can be mono- or multi-exponential. In the case of a multi-exponential lifetime, 'apparent fluorescence lifetime' is the mono-exponential decay that best fits the fluorescence decay.

As for steady-state fluorescence, the FLT assay can be based on endogenous fluorescence. It has been reported in the literature that the FLT of certain native tissues is altered according to the degree of malignancy in the tissues. Fluorescence at 340 nm (possibly due to tryptophan) shows a double-exponential decay with both a short and a long lifetime, and the intensity ratio between them changes from benign tissue to malignant tumour (increase of the apparent FLT) (13). This is possibly due to changes in the micro-environment (14). Changes in FLT of NADH between the free form (0.4 ns) and the protein-bound form (1.0 ns) have also been reported (15).

Contrast can also be achieved on the basis of exogenous fluorochromes (16). The lifetime of certain photosensitizers is sensitive to the local micro-environment (17, 18), and is therefore altered between normal and diseased tissue.

A change in the apparent lifetime of the tissue can also arise if the relative concentration of the fluorochromes having a different lifetime is modified.

PRINCIPLES

Several standard methods are available to measure short light pulses (in the range of the ns) such as time-correlated single photon counting, time-gated integration, streak scope etc. However, the wish to produce images rather than single spot measurements has directed the authors' choice to the so-called 'frequency-domain fluorescence lifetime imaging' (FD-FLIM) (19). Imaging is preferable as it is more compatible with clinical endoscopy.

The principle of frequency-domain FLT measurement has been widely discussed in the literature (16, 20–22). In short, it consists in modulating the excitation light and measuring the phase shift or the demodulation of the fluorescence from which the FLT can be deduced. This phase shift and demodulation occur due to the non-zero FLT of fluorochromes that act as a first-order low-pass filter. Although the fluorescence decay of most fluorochromes (and therefore of a mixture of fluorochromes) is usually multi-exponential, the measurement at one frequency allows the
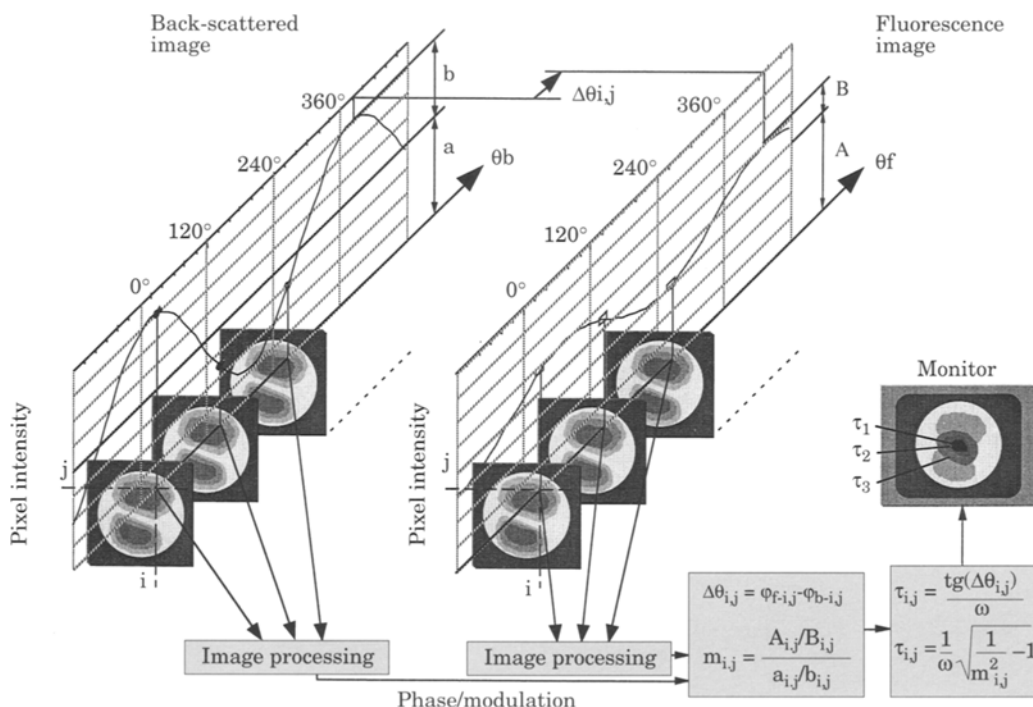
Fig. 1. Frequency-domain fluorescence lifetime imaging principle. An intensity image (frame) is recorded at a fixed relative phase between excitation and detection (homodyne detection). The relative phase is then changed by 120° and a second frame is recorded. With three successive frames, the phase of the fluorescence can be calculated, pixel by pixel, by cosine transform. A second channel (back-scattered light) is recorded following the same procedure and serves as a reference. The absolute phase shift (difference between fluorescence and back-scattered phases) or demodulation enables calculation of the apparent fluorescence lifetime of the corresponding pixel.

determination of only one FLT, which is the 'apparent FLT'.

With the frequency-domain technique, the quantity measured (phase of the fluorescence signal) is not absolute but depends on the excitation modulation. Therefore, one generally speaks in term of phase shift (phase added by the emission delay) or demodulation (loss of modulation due to emission delay). The absolute values of the phase and modulation are difficult to measure in the clinical context. The path length of the excitation and fluorescence photons changes from one endoscope to another, between the centre and the side of the image and with the geometry of the organ investigated. Moreover, the electro-optic modulators are usually not stable in phase and modulation depth (temperature drift), and these may both change during the examination. To correct for all these artefacts, two images were taken in two different spectral windows. One is an image of the excitation light back-scattered by the tissue and is considered as the reference image (zero-delay image). The second is the fluorescence image itself, which contains the information about the phase shift and the demodulation (Fig. 1).

INSTRUMENTATION

The FD-FLIM instrumentation has been described in detail elsewhere (20, 23). Briefly, it measures the apparent fluorescence lifetimes of an endoscopic image in real time (quasi-video rate), pixel by pixel. The result is displayed in colour for direct evaluation by the physician during the endoscopic examination. Conventional white light images can also be displayed at any time on the same screen (Fig. 2).

The excitation is provided by a continuous wave (CW) laser (Ar+, Kr+ or dye-laser) modulated in amplitude by an electro-optic modulator (Quantum Technology, Lake Mary, FL, USA: model 27 and driver 3500). The modulated light is transmitted to the endoscopic site through an optical fibre. The tissue fluorescence is excited and its image is transmitted through the optics of the endoscope (rigid or fibrescope) towards the photocathode of an image intensifier (Hamamatsu, Hamamatsu City, Japan: V5548). The gain of the image intensifier is modulated between the photocathode and the micro-channel plate at the same frequency as the excitation light, and the
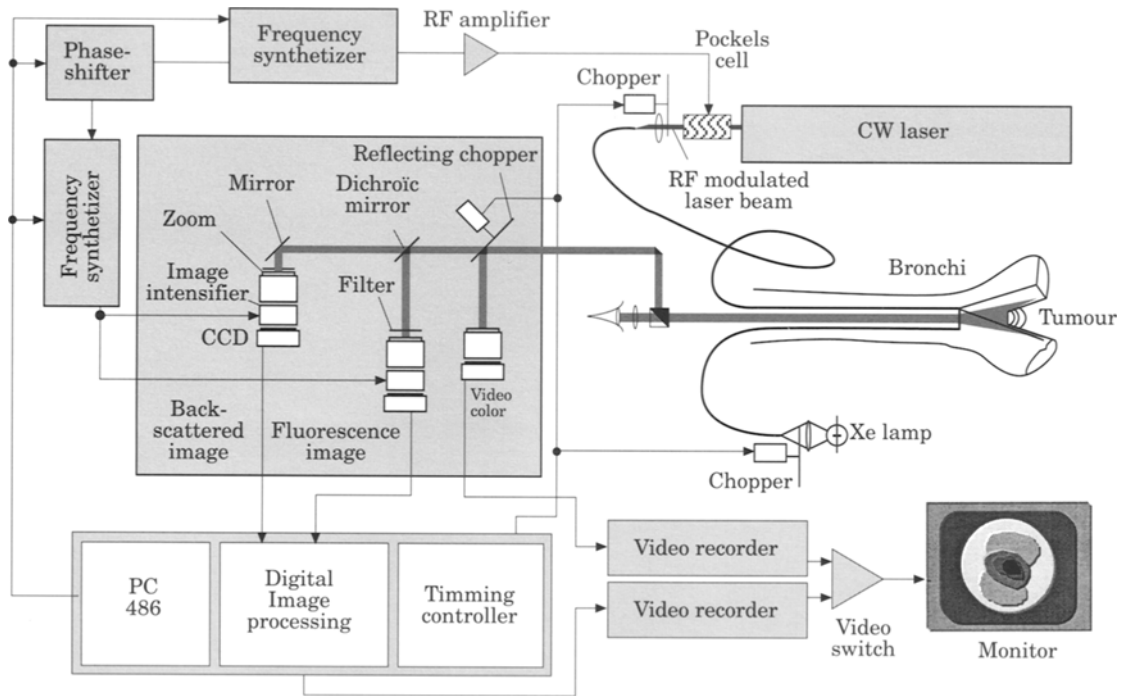
Fig. 2. Instrumentation set-up. Illumination is provided by a continuous wave (CW) laser modulated by an electro-optic modulator. The endoscopic image is split in two spectral windows (excitation and fluorescence) and recorded by intensified CCDs. The gain of the image intensifiers is modulated for homodyne detection. Standard white light endoscopy can also be performed by switching to a Xe lamp and a colour CCD camera.

phase between those two modulations can be adjusted by a phase-shifter (Merrimac, West Caldwell, NJ, USA: PSE-4-10B). The resulting steady-state fluorescence image is recorded by a CCD camera (Hamamatsu, Hamamatsu City, Japan: C5985).

The image of the back-scattered light is recorded by a second image intensifier and CCD camera. The phase shift and demodulation of the fluorescence signal is measured with respect to the back-scattered image (zero-delay image). Acquisitions of the fluorescence and back-scattered channels are performed simultaneously. The relative phase and modulation of the fluorescence signal is then calculated by Fourier transform, using an image processing board (LSI, UK: PCI/C80) on a PC (Pentium 133 MHz). The lifetime image can be acquired, computed and displayed in real time (video rate=40 ms). However, the acquisition time can be increased (typically 120 or 200 ms) in order to reduce the shot noise (on-chip integration).

Although the information given by this instrumentation concerns principally the FLT of the fluorochromes, the fluorescence intensity still provides valuable information. Both are displayed on the same image following the rules of the Hue-Saturation-Lightness (HSL)

coding of colours (24, 25). The FLT is represented as the hue of the corresponding pixel, and the intensity of the fluorescence is represented as the lightness of the pixel (the saturation being kept at 100%).

The short lifetimes are displayed in blue and the long lifetimes in red, whereas the mid-range lifetimes are displayed in green where the light sensitivity of the eye is the best. Due to the non-linearity of the light sensitivity of the eye, a gamma curve ($\gamma = 0.5$) was adopted in order to linearize the perception of the intensity.

COMPUTER SIMULATION

When applied to biological samples, the accuracy of the FLT determined with frequency-domain techniques depends on several factors, such as the type of signal processing (phase or modulation), the modulation frequency, the noise on the fluorescence signal and the tissue optical properties. The effect of each of these has been evaluated by computer simulation and analytical studies in order to optimize the parameters for this application.

The optimal frequency of modulation depends on several factors, including the value

of the lifetime to be measured, the influence of the shot noise and the tissue optics. In a first approximation, the value of the angular frequency ($\omega = 2\pi f$) should be roughly the inverse of the lifetime to be measured.

The shot noise is the limiting factor for fluorescence imaging as the amount of fluorescence photons is determined by the acquisition time, the illumination intensity and the fluorescence quantum yield, and they are distributed on to the thousands of pixels of the detector. For endoscopic imaging, this is even more critical due to the poor optical efficiency of standard medical endoscopes (mainly due to the small aperture of their lenses). The influence of the shot noise changes with the frequency so that there is an optimal modulation frequency for which the standard deviation of the FLT measured is minimal.

It has been shown by computer simulation and analytical study (23) that the shot noise has a minimal influence at frequencies slightly below $1/(2\pi\tau)$ when measuring the lifetime using the phase shift, and at frequencies slightly higher than $1/(2\pi\tau)$ when measuring the lifetime using the demodulation. The influence of the shot noise can be reduced by increasing the number of photons per pixel and per frame by increasing the acquisition time (on-chip integration) or decreasing the size of the image on the CCD. The latter causes an inherent loss of resolution. The number of photons per frame (one phase) and per pixel should not be below a few thousand to measure an FLT between 1 and 10 ns with a standard deviation of 1 ns at frequency of typically 40 MHz.

One of the variable parameters of FD-FLIM instrumentation is the number of phases at which the images are acquired. It has been shown previously that this number does not dramatically affect the noise of the calculation due to the shot noise for a given total acquisition time (ie time per frame multiplied by the number of frames per cycle of acquisition) (23). Therefore, the present authors have chosen a cycle of acquisition of three images only, with a phase of 120° between them to determine the three unknown parameters, ie the phase, the modulation amplitude and the offset. The electronic and numeric part of the instrumentation is therefore simplified.

The tissue optical properties also have an influence on the calculated values of the FLT, due to the time-of-flight of the excitation and emission photons in the tissue. Those times-of-
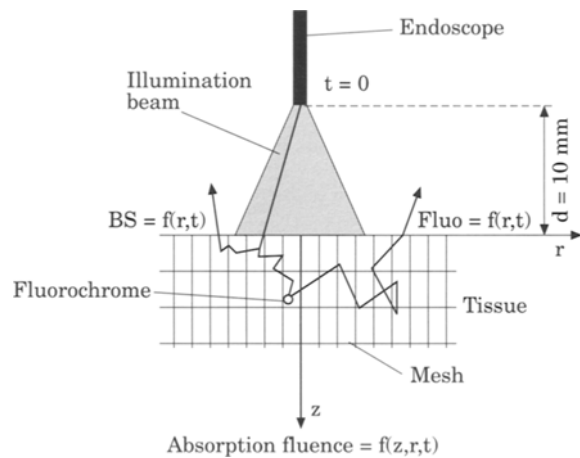

Fig. 3. Geometry of the Monte-Carlo simulation. The endoscope is 10 mm away from the tissue. The illumination is provided by an optical fibre. Times-of-flight of the photons are calculated from exiting the illumination bundle of the endoscope.

flight are added to the delay of fluorescence and therefore affect the measurement of the phase shift. The influence of the tissue optics is greater at high frequencies and when the tissue is less absorbent because the duration of the photon path becomes longer in comparison to the inverse of the frequency.

A Monte-Carlo simulation program has been developed in order to estimate the error due to this effect. It is based on an original code written by L. Wang and S. Jacques (26), and enables the simulation of the path of both the excitation and the fluorescence photons within the tissue.

The delay of the fluorescence emission (FLT) can be introduced directly in the program (random emission delay with an exponential distribution and a mean value equal to the FLT) or calculated by convolution of the impulse response of the tissue with the temporal function of the fluorescence (exponential decay) after the simulation. The latter is faster and is usually employed. In the same way, the temporal function of the source (sine wave) is convoluted after the simulation. Alternatively, the frequency response can be calculated at all frequencies by Fourier transform of the temporal impulse response of the tissue.

The particular geometry of endoscopic imaging (illumination by an optical fibre: not homogeneous, not infinite and not perpendicular to the tissue; Fig. 3) can be simulated directly with no need for subsequent spatial convolution.

Therefore, one can directly simulate the fluorescence emitted from the surface of the
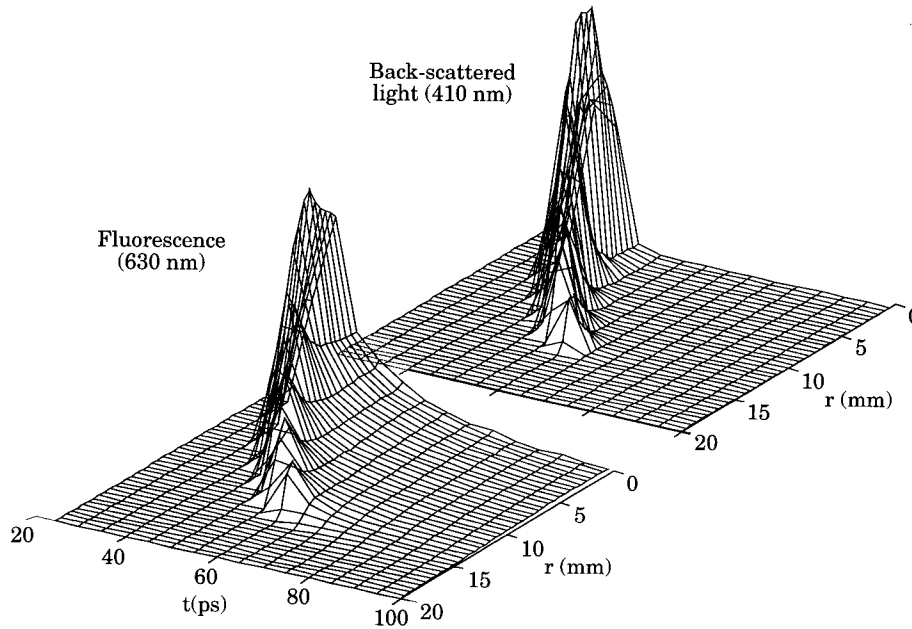
Fig. 4. Time-of-flight of the excitation and fluorescence photons; optical parameters: excitation (410 nm): μ_a=24 cm^{-1}, μ_s=714 cm^{-1}, g=0.7; fluorescence (630 nm): μ_a=0.9 cm^{-1}, μ_s=100 cm^{-1}, g=0.7; origin of times: distal end of the endoscope (10 mm away from the tissue); the temporal axis shows the time at which the photon exits the tissue.

tissue as a function of the time and the distance from the optical axis of the system. The time-of-flight of the photons is measured from their launch at the endoscope's distal end (illumination fibre optic) to their exit from the tissue. The time-of-flight of the fluorescence photon is added to the time-of-flight of the excitation photon so that the origin of the times is the same for all the photons.

RESULTS AND DISCUSSION

The results of the Monte-Carlo simulation are shown in Fig. 4 for the typical excitation and emission wavelengths of porphyrins. The longest times-of-flight are typically 5–10 ps for the excitation light (410 nm) and 20–30 ps for the fluorescence (630 nm). For the simulation, the FLT was set to 0. Therefore, the difference of the times shown is only due to the difference of path length of the excitation and fluorescence photons. Figure 4 also illustrates the strong inhomogeneity of illumination with an optical fibre.

The fluorescence result was convoluted with two FLTs (100 ps and 1 ns), and the response to a sinusoidal excitation was then calculated by Fourier transform for frequencies up to 1 GHz by steps of 100 MHz. This gives a fluorescence modulation equivalent to the one exiting from the tissue surface. Then, the FLTs were

calculated by the algorithm of the instrumentation (using the phase shift) and compared to the theoretical values. Table 1 shows these values for the first element of the spatial grid (axis of the endoscope).

The time-of-flight of the photons within the tissue affects the deduced value of the FLT by an amount which is proportional to the frequency multiplied by the FLT (same value of 22 ps for a FLT of 100 ps at 977 MHz or for a FLT of 1 ns at 97.7 MHz). Hence, the influence of the time-of-flight is proportionally smaller for longer FLT.

Another interesting result is that the accuracy of the calculation of the FLTs decreases when the frequency becomes higher. This is due to the fact that when the phase shift is approaching $-90°$, the function of the lifetime vs the phase shift becomes steeper and a small increase in phase dramatically affects the calculated lifetime.

Furthermore, the difference of phase shift between the fluorescence and the back-scattered signal depends on the optical properties of the tissue alone, and is linear with the frequency of modulation. In the case of the tissue simulated, the additional phase shift due to the time-of-flight is of 5.5° GHz^{-1}, which corresponds to 15.3 ps or 3.3 mm of optical path within the tissue.

Therefore, for a given tissue and a known frequency of modulation, it is possible to

Table 1. Simulated phase of back-scattered and fluorescence signals compared to the theoretical values; calculated fluorescence lifetime compared to actual values; data are for the first radius grid (r=0.25 mm)

Frequency (MHz)	Absolute fluorescence phase-shift for tau=100 ps (°)			Absolute fluorescence phase-shift for tau=1 ns (°)			Calculated FLT (ps) (tau=100 ps)	Calculated FLT (ns) (tau=1 ns)
	Simul.	Theor.	Difference	Simul.	Theor.	Difference		
97.7	− 4.07	− 3.5	− 0.57	− 32.1	− 31.5	− 0.57	116	1.02
195	− 8.08	− 6.99	− 1.09	− 51.9	− 50.8	− 1.09	116	1.04
293	− 12.1	− 10.4	− 1.66	− 63.1	− 61.5	− 1.66	116	1.07
391	− 16	− 13.8	− 2.18	− 70	− 67.8	− 2.18	117	1.12
488	− 19.8	− 17.1	− 2.75	− 74.7	− 72	− 2.75	117	1.19
586	− 23.5	− 20.2	− 3.27	− 78	− 74.8	− 3.21	118	1.28
684	− 27	− 23.3	− 3.78	− 80.7	− 76.9	− 3.84	119	1.42
781	− 30.5	− 26.1	− 4.35	− 82.8	− 78.5	− 4.33	120	1.61
879	− 33.8	− 28.9	− 4.87	− 84.6	− 79.8	− 4.85	121	1.91
977	− 36.9	− 31.5	− 5.39	− 86.1	− 80.7	− 5.36	122	2.4

correct the fluorescence phase shift (and the FLT calculated) for one fluorescence wavelength.

Before being used in a clinical environment, the instrumentation was set up on an optical bench. Measurements were performed on several human tissue samples, comprising oral mucosa and urinary bladder. Different excitation wavelength and fluorescence spectral windows were investigated, depending on the fluorochrome of interest. The FLTs were calculated using the phase shift. For the two cases reported below, no exogenous fluorochromes were added.

Figure 5 shows a resected human urinary bladder, which had been opened along its median axis. On the left is a standard white light video print showing the urothelium. One can see a dark invasive tumour on the right lower corner, surrounded by a reddish disc of erythematous urothelium. The other part of the urothelium is normal. The image on the right is the fluorescence lifetime image of the same tissue. The colour of each pixel represents the apparent FLT between 0 ns (blue) and 4 ns (red), while the intensity represents the intensity of fluorescence (γ coefficient: 0.25). The excitation wavelength was 363 nm (med-UV Ar+ laser) and the detection window extends from 470 to 650 nm. The frequency of modulation was 40 MHz.

The healthy mucosa fluoresces with an apparent lifetime of 2.6 ± 0.2 ns (yellow), the erythematous urothelium with an apparent lifetime of 1.65 ± 0.4 ns (green) and the ulcerated tissue with an apparent lifetime of 1.25 ± 0.4 ns (blue). In this example, the

fluorescence probably comes from NADH ($\lambda_{exc.}$=363 nm). The lifetime, as well as the intensity, decreases in the erythema and in the diseased tissue.

Figure 6 shows a sample of oral mucosa after CO_2 laser resection. The colour of each pixel represents the apparent FLT between 0 ns (blue) and 5 ns (red), and the intensity represents the intensity of fluorescence (γ coefficient: 0.5). The excitation wavelength was 417 nm (Ar+ pumped dye laser—stilben 1) and the detection window extended from 470 to 650 nm. The frequency of modulation was 40 MHz.

The normal mucosa fluoresces with an apparent lifetime of 2.5 ± 0.2 ns (green), while the area in the middle shows an increase of the FLT up to 3.44 ± 0.7 ns (red). This area was diagnosed as a carcinoma in situ with spots of micro-invasion. In this case, the fluorescence comes from a mixture of fluorochromes but the contribution of the porphyrins is probably enhanced due to the excitation wavelength (417 nm). The lifetime image suggests that the concentration of porphyrins increases in CIS, resulting in an increase of the apparent FLT due to the long FLT of the porphyrins.

CONCLUSION

Fluorescence lifetime images of human tissue samples were successfully performed. The fluorescence lifetime alters between healthy and pathologic tissue. When excited at 363 nm, the FLT of pathologic tissues tends to decrease, whereas the opposite occurs when
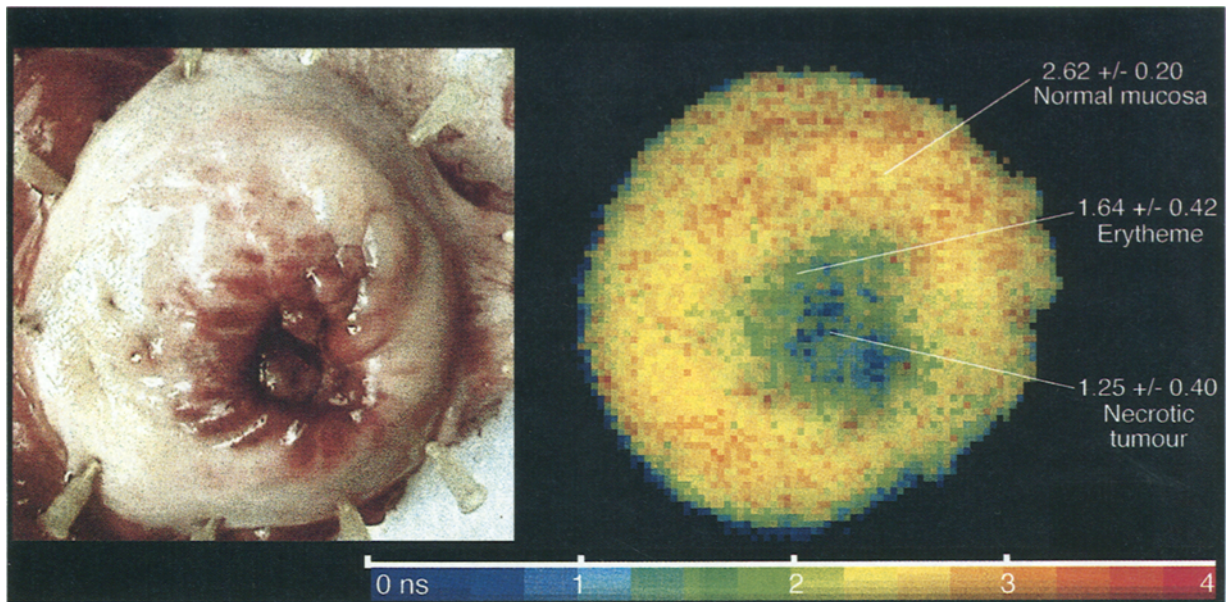
Fig. 5. Excised human urinary bladder cut and opened along its median axis. Size of the sample: Ø≈120 mm. *Left:* standard white light videoprint; *right:* fluorescence lifetime image calculated using the phase shift; parameters: $\lambda_{exc.}$=363 nm, $\lambda_{det.}$=470–650 nm, f=40 MHz.
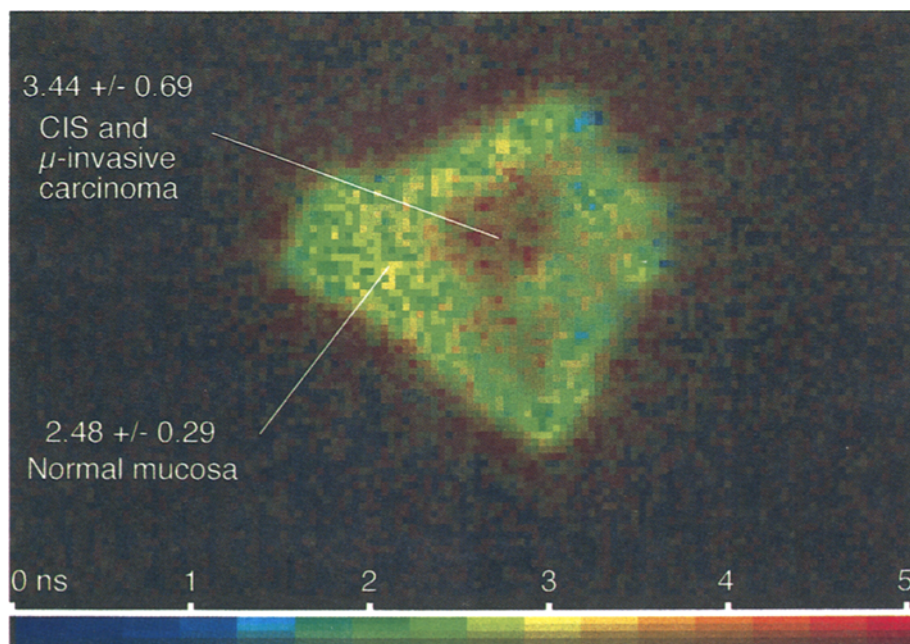

Fig. 6. Excised human oral mucosa; size of the sample: 20×30 mm; fluorescence lifetime image calculated using the phase shift; parameters: $\lambda_{exc.}$=417 nm, $\lambda_{det.}$=470–650 nm, f=40 MHz.

excited at 417 nm. In the bladder case, the contrast may come from an alteration of the NADH molecule (probably to NAD), while in the second case, the contrast may arise from an increase in concentration of the porphyrins within the tumour.

The number of fluorescence photons per pixel and per frame (typically a few thousand)

of the image in Figs 5 and 6 is of the same order of magnitude as expected with Hopkins endoscope with an integration time of 120 ms frame^{-1} and a reduced image size (128 × 128 pixels). Therefore, the temporal resolution of the instrumentation is sufficient for the biological samples investigated (SD around 0.5 ns; dynamic: 1–10 ns) at 40 MHz.

The influence of the tissue optics is a limiting factor only at high frequencies (>GHz) or for short lifetime fluorochromes. Therefore, the calculation using the phase shift is preferable due to the fact that the optimal frequency (in order to minimize the shot noise) is lower (by typically one octave) than the demodulation-based methods. Furthermore, it is easier to modulate the excitation light and the gain of the image intensifier at lower frequencies. Other optical components can also present limitations at high frequencies (like temporal dispersion in the optical fibres).

The error due to the tissue optics can be corrected to a certain extent providing that the optical parameters are known for both fluorescence and excitation wavelengths. This correction can be made for one fluorescence wavelength only.

REFERENCES

1 Jichlinski P, Forrer M, Mizeret J et al. Usefulness of fluorescence photodetection of neoplastic urothelial foci in bladder cancer following intravesical instillation of delta-aminolevulinic acid (5-ALA). San Jose, CA, USA. *SPIE* 1996, **2671**:340–347

2 Lam S, Hung J, Palcic B. Detection of lung cancer by ratio fluorimetry with and without Photofrin II. *Opt Fib Med V* 1990:561–8

3 Schomacker KT, Frisoli JK, Compton CC et al. Ultraviolet laser-induced fluorescence of colonic tissues: basic biology and diagnostic potential. *Lasers Surg Med* 1992, **12**:63–78

4 Harries ML, Lam S, Macaulay C, Qu JA, Palcic B. Diagnostic-imaging of the larynx—autofluorescence of laryngeal tumors using the helium cadmium laser. *J Laryngol Otol* 1995, **109**:108–10

5 Wagnières G, Depeursinge C, Monnier P et al. Photodetection of early cancer by laser-induced fluorescence of a tumor selective dye: Apparatus design and realization. *SPIE* 1990, **1203**:43–52

6 Profio AE. Laser excited fluorescence of hematoporphyrin derivative for diagnosis of cancer. *IEEE J Quant Electronics* 1984, **CIO-20**:1502–7

7 Profio AE, Balchum OJ, Lam S. Endoscopic fluorescence detection of early lung cancer. Optical methods for tumor treatment and early diagnosis: mechanisms and techniques. *SPIE* 1991, **1426**:44–6

8 Monnier P, Savary M, Fontolliet C et al. Photodetection and photodynamic therapy of 'early' squamous cell carcinomas of the pharynx, oesophagus and tracheo-bronchial tree. *Lasers Med Sci* 1990, **5**:149–69

9 Andersson-Engels S, Ankerst J, Montan S, Svanberg K. Aspects of tumour demarcation in rats by means of laser-induced fluorescence and haematoporphyrin derivatives. *Lasers Med Sci* 1988, **3**:239–47

10 Baumgartner R, Fisslinger H, Jocham D et al. A fluorescence imaging device for endoscopic detection of early stage cancer—instrumental and experimental studies. *Photochem Photobiol* 1987, **46**:759–63

11 Lam S, Hung J, Palcic B. Mechanism of detection of early lung cancer by ratio fluorimetry. *Lasers Life Sci* 1991, **4**:67–73

12 Sinaasappel M, Sterenborg HJCM. Quantification of the hematoporphyrin derivative by fluorescence measurement using dual-wavelength excitation and dual-wavelength detection. *Appl Opt* 1993, **32**:541–8

13 Pradhan A, Das BB, Yoo KM et al. Time-resolved UV photoexcited fluorescence kinetics from malignant and non-malignant human breast tissues. *Lasers Life Sci* 1992, **4**:225–34

14 Schneckenburger H, Seidlitz HK, Eberz J. New trends in photobiology—Time-resolved fluorescence in photobiology. *J Photochem Photobiol B: Biol* 1988, **2**:1–19

15 Lakowicz JR, Szmacinski H, Nowaczyk K, Johnson ML. Fluorescence lifetime imaging of free and protein-bound NADH. *Biochemistry* 1992, **89**:1271–5

16 Schneckenburger H, König K, Kunzi-Rapp K, Westphal-Frösch C, Rück A. Time-resolved in-vivo fluorescence of photosensitizing porphyrins. *J Photochem Photobiol B: Biol* 1993, **21**:143–7

17 Wagnières G, Iinuma S, Schomacker KT, Deutsch T, Hasan T. In-vivo tissue characterization using environmentally sensitive fluorochromes. *Fluoresc Microsc Fluoresc Probes* 1996:203–9

18 Zhang JZ, O'Neil RH, Evans JE. Femtosecond studies of hematoporphyrin derivative in solution: effect of pH and solvent on the excited state dynamics. *Photochem Photobiol* 1994, **60**:301–9

19 Lakowicz JR, Szmacinski H, Nowaczyk K, Berndt KW, Johnson ML. Fluorescence lifetime imaging. *Anal Biochem* 1992, **202**:316–30

20 Wagnières G, Mizeret J, Studzinski A, van den Bergh H. Endoscopic frequency-domain fluorescence lifetime imaging for clinical cancer photodetection: apparatus design. In: Dougherty TJ (ed.) *Optical Methods for Tumor Treatment and Detection: Mechanisms and Techniques in PDT IV*. San Jose. *SPIE* 1995, **2392**:42–54

21 Lakowicz JR. *Principles of Fluorescence Microscopy*. New York: Plenum Press, 1983

22 Jameson DM, Gratton E, Hall R. The measurement and analysis of heterogeneous emission by multifrequency phase and modulation fluorometry. *Appl Spectrosc Rev* 1984, **20**:55–106

23 Mizeret J, Wagnières G, Studzinski A, Shangguan C, van den Bergh H. Endoscopic tissue fluorescence life-time imaging by frequency-domain light induced fluorescence. *Optical biopsies*. Barcelona, Spain. *SPIE* 1995, **2627**:40–8

24 MacAdam DL. *Color Measurement*. Berlin: Springer-Verlag, 1985

25 Kowaliski P. *Vision de la Couleur*. Paris: Masson, 1990

26 Wang L, Jacques S-L. Monte-Carlo Modeling of Light Transport in Multilayered Tissues in Standard C. Houston: University of Texas, 1992